Light-assisted electrocatalytic PMS activation system based on Co_3O_4-SnO_2/NF cathode for efficient degradation of tetracycline over wide pH conditions

Jiaxuan Wei[a, 1], Yue Hou[a, 1], Zhaodi Zhang[a], Shuangshuang He[a], Yufei Li[a], Yuanzhen Zhou[a,b], Kangkang Wang[a,*], Zhen Wang[a,b,*], Yuan Dang[a,b,*]

a School of Chemistry and Chemical Engineering, Xi'an University of Architecture and Technology, Xi'an, 710055, China

b Engineering Research Center of Low-Carbon Energy Efficient Utilization, Universities of Shaanxi Province, School of Chemistry and Chemical Engineering, Xi'an University of Architecture and Technology, Xi'an, 710055, China

[1]The authors contribute equally in this work.

*Corresponding author at: School of Chemistry and Chemical Engineering, Xi'an University of Architecture and Technology, No. 13, Yanta Road, Xi'an, Shaanxi Province, China.

E-mail addresses: dangy_0920@126.com, dangyuan@xauat.edu.cn (Y. Dang);

xjd-wangzhen@xauat.edu.cn (Z. Wang)

kangkangw@xauat.edu.cn (K. Wang)

Contents of supplementary file

Text S1

The process efficiency can be evaluated by the electrical energy per order (EE/O). EE/O represents the electrical energy required to reduce the pollutant concentration by one order of magnitude in 1 m^3 of wastewater and serves as an important indicator for assessing the energy consumption level of the degradation process, as shown in Eq (1).

$$EE/O\ (KW \cdot h \cdot m^{-3}) = \frac{U \times I \times t}{V \times log(C_0/C_t)} \quad (1)$$

Text S2

The formation rate of $^1O_2$ in electrochemical system was determined by reaction rate of between FFA and $^1O_2$ (k_{1O2}, FFA = 1.2×10^8 M^{-1} s^{-1}). The steady-state concentration of $^1O_2$ ($[^1O_2]_{ss}$) can be determined by dividing the observed FFA degradation rate by the biomolecular reaction rate constant of FFA with $^1O_2$ according to Eq. (2).

$$[^1O_2]\text{ss} = \frac{\ln\left(\frac{FFA_0}{FFA_t}\right)}{dt\ k_{1O2}} \quad (2)$$

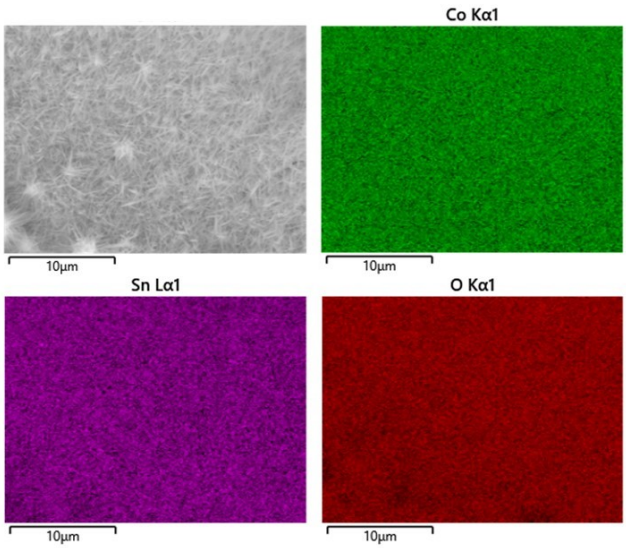

Fig. S1 Mapping images of Co and Sn of Co_3O_4-SnO_2/NF.

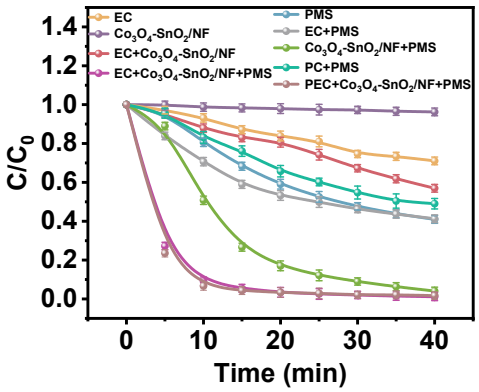

72

73 Fig. S2 Comparison of TC removal effects in different systems.

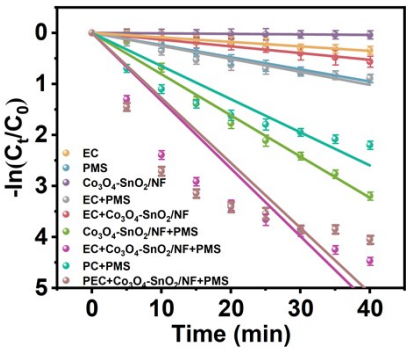

74

75 Fig. S3 The corresponding kinetic curves in different systems.

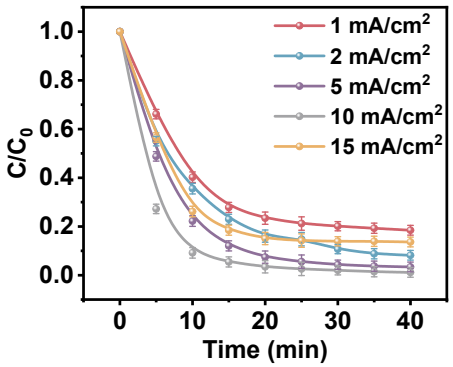

Fig. S4 Removal of TC in EC+ Co_3O_4-SnO_2/NF + PMS system with different current density (nature pH, PMS = 2 mM, T = 25℃).

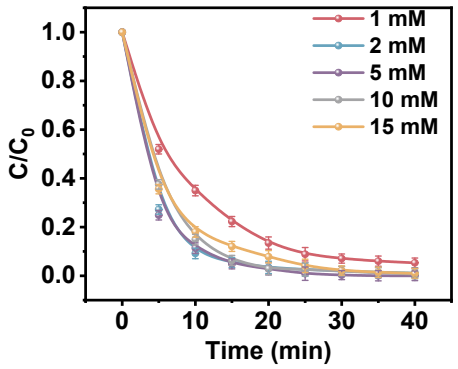

79

80 Fig. S5 Removal of TC in EC+ Co_3O_4-SnO_2/NF + PMS system with different PMS

81 dosage (j = 10 mA/cm^2, nature pH, T = 25℃).

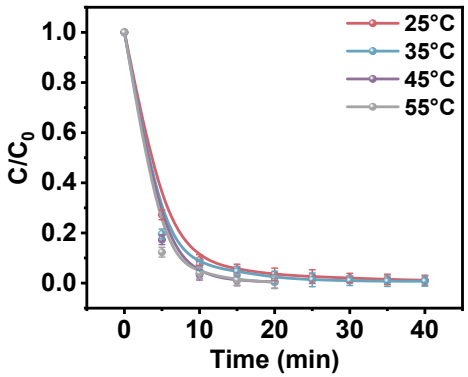

82

83 Fig. S6 Removal of TC in EC+ Co_3O_4-SnO_2/NF + PMS system with different

84 temperature (j = 10 mA/cm^2, nature pH, PMS = 2 mM).

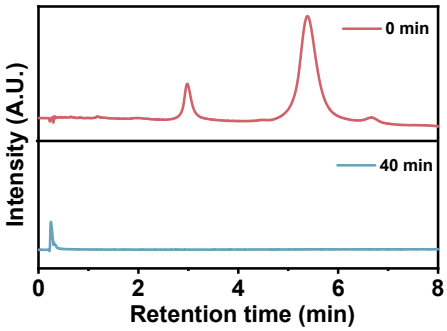

Fig. S7 HPLC chromatograms of TC before and after degradation in the PEC+Co_3O_4-SnO_2/NF +PMS system.

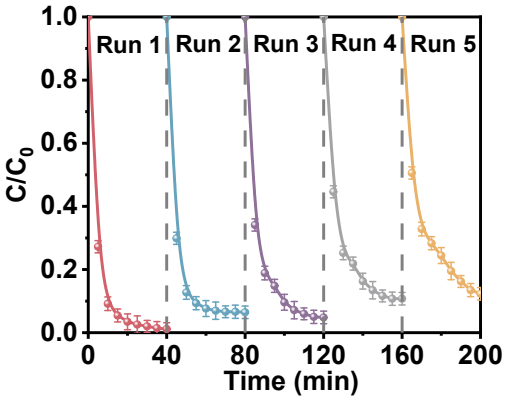

88

89 Fig. S8 Stability of the Co_3O_4-SnO_2/NF cathode during TC degradation.

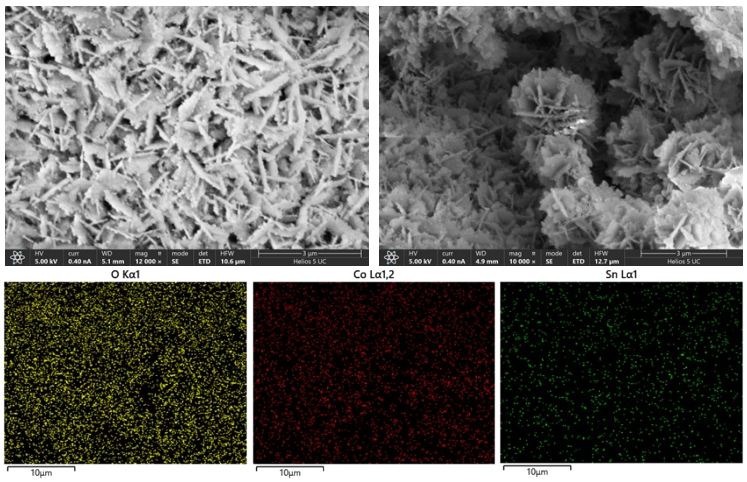

Fig. S9 SEM images and elemental mapping of the Co_3O_4-SnO_2/NF after five degradation cycles.

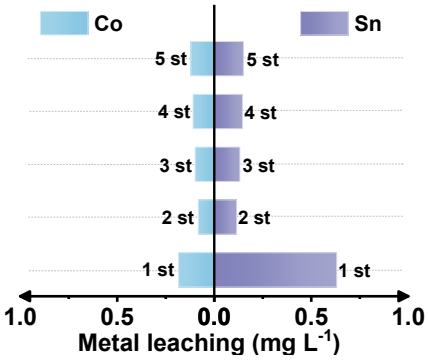

93

94 Fig. S10 Concentrations of leached Co and Sn after five cycles.

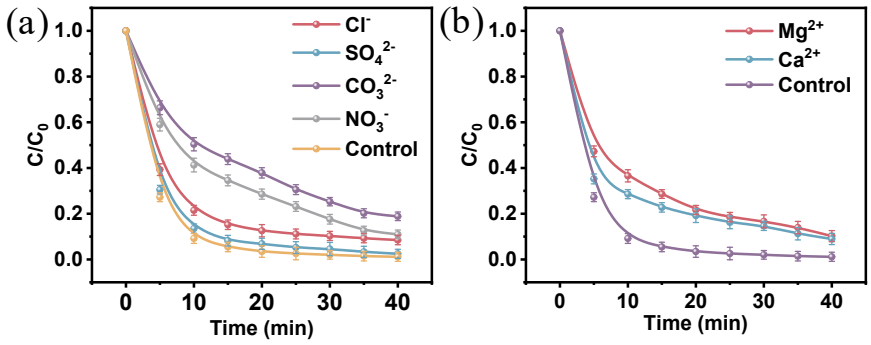

Fig. S11 The effect of co-existing (a) anions and (b) cations on TC degradation in the PEC+Co_3O_4-SnO_2/NF+PMS system.

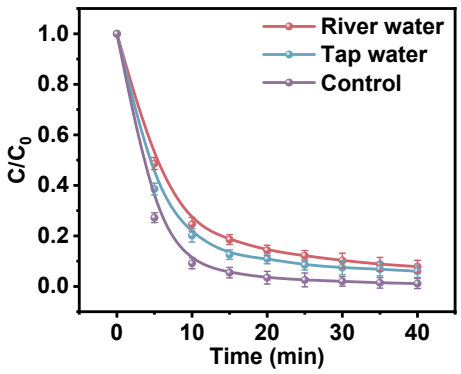

98

99 Fig. S12 The removal efficiencies of TC spiked in the tap water and river water using

100 the PEC+Co_3O_4-SnO_2/NF+PMS system.

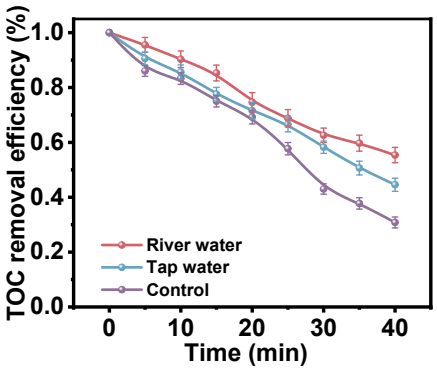

101

102 Fig. S13 TOC removal efficiency of the PEC+Co_3O_4-SnO_2/NF+PMS system in real

103 water matrices.

104

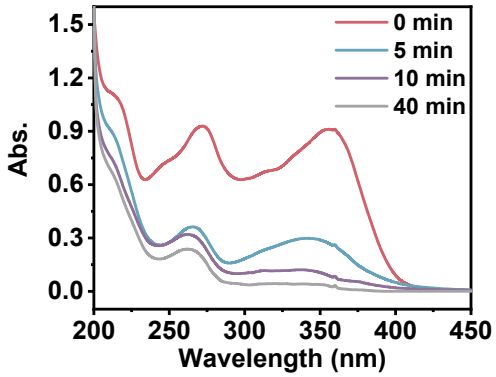

105

106 Fig. S14 UV-vis spectra at 200-450nm in PEC+ Co_3O_4-SnO_2/NF + PMS system.

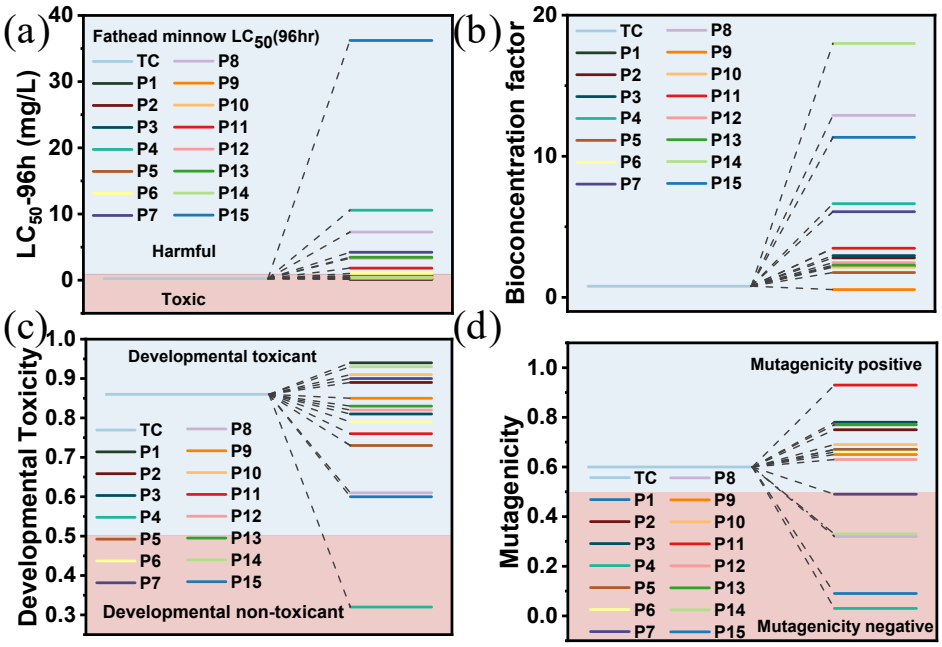

107

108 Fig. S15 Toxicity assessment (a) Fathead minnow LC50 (96 hr). (b) Bioconcentration

109 factor. (c) Developmental toxicity. (d) Mutagenicity.

Table S1 HPLC analysis method for different target pollutants.

Target pollutant	Wavelength (nm)	Temperature (℃)	Flow rate (mL/min)	Mobile phase A	Mobile phase B
TC	350	34	0.5	40 % Methanol	60% 0.1% formic acid
FFA	220	32	0.8	20% Methanol	80% H_2O

Table S2 Estimated mass loading of Co_3O_4-SnO_2 composite on NF

Oxide	Wt% (from EDS)	Mass (mg)	Mass loading ($mg \cdot cm^{-2}$)
Co_3O_4	65.8%	33.1	3.31
SnO_2	34.2%	17.2	1.72
Total	100%	50.3	5.03

Table S3 Specific surface area and pore size of SnO_2/NF, Co_3O_4/NF and Co_3O_4-SnO_2/NF samples.

Sample	BET surface area (m^2/g)	Pore size (nm)
SnO_2/NF	40.5003	10.33150
Co_3O_4/NF	23.5939	21.12187
Co_3O_4-SnO_2/NF	58.3989	7.61836

Table S4 Pseudo-first-order kinetic parameters (k and R^2) for TC degradation in different systems.

System	k (min^{-1})	R^2
EC+Co_3O_4-SnO_2/NF	0.0116	0.9931
PMS	0.0245	0.9775
Co_3O_4-SnO_2/NF	0.0011	0.9659
EC+PMS	0.0335	0.9972
EC	0.0085	0.9883
PC+PMS	0.0649	0.9582
Co_3O_4-SnO_2/NF+PMS	0.0823	0.9684
EC+Co_3O_4-SnO_2/NF+PMS	0.1925	0.9741
PEC+Co_3O_4-SnO_2/NF+PMS	0.1828	0.9825

Table S5 Pseudo-first-order kinetic parameters (k and R^2) for TC degradation in the EC+PMS+Co_3O_4-SnO_2/NF system under different pH conditions.

pH	k (min^{-1})	R^2
3	0.1783	0.9885
5	0.1512	0.9530
Natural pH (5.8)	0.1925	0.9741
7	0.1769	0.9850
9	0.1329	0.9558
11	0.0785	0.9676

Table S6 Comparison of EE/O values with other reported PMS-activation systems

Process	EE/O (kWh m^3 $order^{-1}$)	References
E-PMS-O_3	4.338	(Xue et al. 2024)
E/SC-BN/PMS	3.26	(Zhao et al. 2025)
E/Ce(IV)/PMS	3.27	(Liu et al. 2023)
EC/$CoFe_2O_4$/PMS	2.51	(Zhang et al. 2022)
EC+Fe_3O_4-CaO_2/NF+PMS	0.76	(Zhao et al. 2025)
PEC+Co_3O_4-SnO_2/NF+PMS	0.6443	**This study**

Reference

Xue, Q., Yu, B., Dagnew, M., Li, W., Ding, H., Zhang, J., Sun, Z., Wang, P. and Zhao, C. (2024) Rapid in situ regeneration of phenol-saturated activated carbon fiber by an electro-permonosulfate-ozone process: Performance, operators and mechanism. J. Environ. Chem. Eng. 12(1). http://10.1016/j.jece.2024.111932.

Zhao, Q., Liu, D., Wu, Y., Zhou, L., Lu, S., Lei, J., Zhang, J. and Liu, Y. (2025) An efficient multi-path to active peroxymonosulfate by carbon and sulfur co-doped boron nitride for antibiotics degradation: An emerging electron-transfer pathway at activated-S sites. Sep. Purif. Technol. 352. http://10.1016/j.seppur.2024.128089.

Liu, J., Zhang, X., Li, J., Feng, Y., Feng, L., Han, S., Pan, T., Zhang, T., Wu, S., Ke, Z., Liu, B. and Zheng, H. (2023) Study on the performance efficiency, mechanism, power consumption and biochemical properties of E/Ce(IV)/PMS on the enhanced removal of RB19. Environ. Res. 232, 116271. http://10.1016/j.envres.2023.116271.

Zhang, Q., Sun, X., Dang, Y., Zhu, J.J., Zhao, Y., Xu, X. and Zhou, Y. (2022) A novel electrochemically enhanced homogeneous PMS-heterogeneous CoFe(2)O(4) synergistic catalysis for the efficient removal of levofloxacin. J. Hazard. Mater. 424(Pt D), 127651. http://10.1016/j.jhazmat.2021.127651.